

## A fluid floating bilayer

G. FRAGNETO<sup>1,2</sup>, T. CHARITAT<sup>3</sup>, F. GRANER<sup>4</sup>(\*), K. MECKE<sup>5</sup>,  
L. PERINO-GALLICE<sup>1,4</sup> and E. BELLET-AMALRIC<sup>1,6</sup>

<sup>1</sup> *Institut Laue-Langevin - B.P. 156, F-38042 Grenoble Cedex, France*

<sup>2</sup> *INFM - Genova, Italy*

<sup>3</sup> *Institut Charles Sadron(\*\*) - 6 rue Boussingault, F-67083 Strasbourg Cedex, France*

<sup>4</sup> *Spectrométrie Physique(\*\*\*) - B.P. 87, F-38402 St Martin d'Hères Cedex, France*

<sup>5</sup> *Bergische Universität Wuppertal, Fachbereich Physik - D-42097 Wuppertal, Germany*

<sup>6</sup> *DRFMC/SP2M/SGX CEA - 17 Avenue des Martyrs, F-38054 Grenoble, France*

(received 13 January 2000; accepted in final form 20 October 2000)

PACS. 87.16.Dg – Membranes, bilayers and vesicles.

PACS. 87.15.Ya – Fluctuations.

PACS. 61.12.Ha – Neutron reflectometry.

**Abstract.** – A highly hydrated lipid bilayer, floating a few Å above another one adsorbed on a smooth solid substrate, was prepared at room temperature where lipids (DSPC) are in gel phase, then heated at several temperatures including the pretransitional temperature  $T_p$  and the chain melting temperature  $T_m$ . A precise *in situ* characterization by neutron reflectivity led to two new results. First, even when in fluid phase the floating bilayer was structured and stable; it thus provides a flexible model system for physical and biophysical studies of membranes. Second, at intermediate temperatures, a spectacular maximum in both inter-bilayer distance and bilayer roughness was simultaneously observed. It might be a direct observation of the balance between energy minimization and entropic repulsion, leading to an estimation of the dimensionless parameter  $(k_B T)^2 / A \kappa$ , where  $A$  is the Hamacker constant and  $\kappa$  the bending modulus.

Biophysical studies of membrane-membrane and membrane-protein interactions require well-controlled model systems [1, 2]. We had already developed a new method to obtain a single *floating* lipid bilayer, fluctuating in excess water in the vicinity of an *adsorbed* bilayer, and characterized it in the gel phase [3]. The floating bilayer has several advantages over existing model membranes [1]. i) The composition of each layer can be controlled: lipid heads and tails, charges, inclusions, as well as purity and absence of solvent residues. ii) Its large size ( $\text{cm}^2$ ) and its well-defined ( $\text{Å}$ ) position with respect to the substrate enable reflectivity studies. iii) Since it is in contact with a semi-infinite water reservoir, it is fully hydrated and free to fluctuate. iv) Its controlled structure remains unchanged for days, indicating a good stability or at least metastability.

---

(\*) E-mail: graner@ujf-grenoble.fr

(\*\*) CNRS-UPR 22.

(\*\*\*) CNRS-UMR 5588, Université Grenoble I.

Here we report two effects of temperature on the floating bilayer: it remained stable even when it became fluid; its distance to the adsorbed bilayer went through a maximum near the melting temperature of the lipid chains.

The substrate was a smooth  $5 \times 5 \text{ cm}^2$  silicon crystal, 1 cm thick, polished at nearly atomic roughness, and highly hydrophilic thanks to an UV/ozone oxidation. A lipid monolayer of DSPC (L- $\alpha$ -Di-stearoyl phosphatidyl-choline, Avanti Polar Lipids) was spread on the water surface of a home-made Langmuir-Blodgett trough at room temperature, and compressed to high surface pressure (40 mN/m). Two vertical depositions, upwards then downwards, resulted in a first adsorbed bilayer. The second floating bilayer was deposited on top of it by a vertical deposition upwards followed by a horizontal (Langmuir-Schaeffer [4]) deposition realized directly onto a PTFE lid full of  $\text{D}_2\text{O}$  (93 % purity); for details see [3]. Transfer ratios for the first layers were 1.0, 0.85 and 0.99 (measured by the displacement of the barrier); for the last layer, it was estimated to be 0.96 (from the 3.6 mN/m overshoot in pressure, the slope of the isotherm, and the ratio of substrate to trough areas).

Neutron reflectivity [5] is an *in situ* non-destructive tool to extract structural information with  $\text{\AA}$  precision. Measurements were performed at the Institut Laue Langevin on the D16 diffractometer. A monochromatic neutron beam ( $\lambda = 4.52 \text{ \AA} \pm 1\%$ ) hit the sample at grazing incidence. The two-dimensional  $^3\text{He}$  detector was kept in a fixed position covering the angular  $2\theta$  range  $0^\circ$ – $9^\circ$ . The beam was vertically focused at the detector position in order to gain

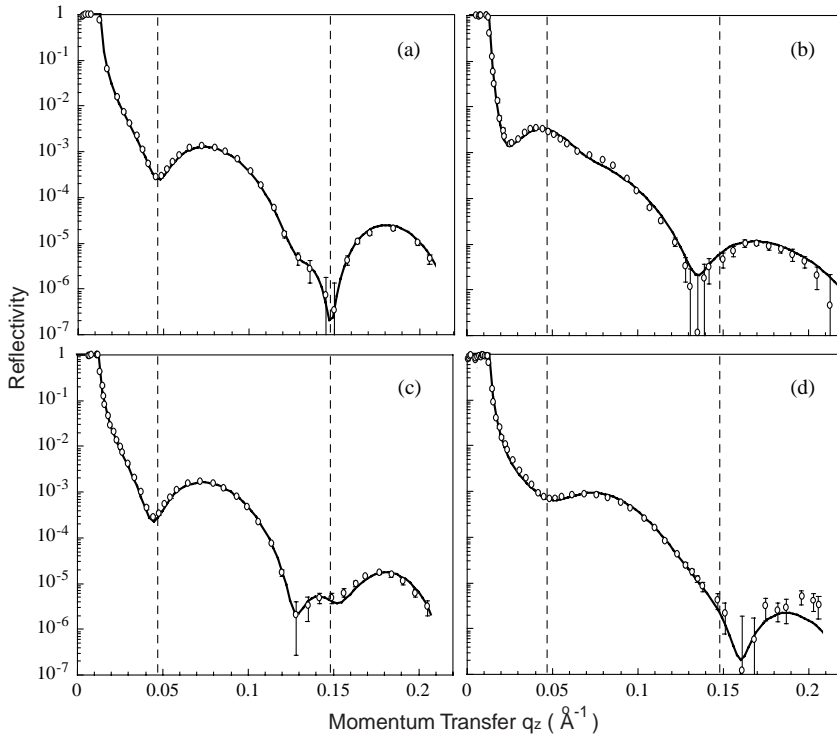


Fig. 1 – Specular reflectivity profile of the double DSPC bilayer in 93%  $\text{D}_2\text{O}$ : (a) gel phase  $T = 25.4^\circ\text{C}$ ; (b) transition region  $T = 51.5^\circ\text{C}$ ; (c) fluid phase  $T = 55.4^\circ\text{C}$ ; (d) high temperature  $T = 64.1^\circ\text{C}$ . Error bars = 99% confidence intervals, see [3]. Solid lines are best fits with parameters listed in table I. To facilitate the comparison, vertical lines indicate the positions of minima in (a).

intensity (flux  $\simeq 2 \cdot 10^6 \text{ cm}^{-2} \text{ s}^{-1}$  at sample position) without worsening divergence. The high flux, a good shielding all along the neutron path, and the use of  $\text{D}_2\text{O}$  as contrast-enhancing subphase enabled to cover a dynamical range greater than  $10^6$  in reflectivity [3].

The neutron reflectivity curves (fig. 1) of the same sample were measured at different temperatures (table I) in the water-regulated sample chamber, monitored with a thermocouple (equilibration time  $\sim 25$  minutes, stability  $< 0.1 \text{ }^\circ\text{C}$ , absolute precision  $< 0.3 \text{ }^\circ\text{C}$ ). Two types of measurements were performed. The whole available  $q$ -range =  $0.003\text{--}0.22 \text{ \AA}^{-1}$  was scanned in eight hours, after one hour equilibration. After a temperature step of 1 or 2  $^\circ\text{C}$ , without equilibration, quick scans ( $\sim 1$  h) were measured in a restricted  $q$ -range =  $0.003\text{--}0.06 \text{ \AA}^{-1}$ .

A reflectivity curve essentially reflects the sample density perpendicular to the substrate surface, or rather the square modulus of its Fourier transform. Since the phase is lost, data need to be fitted (*e.g.*, with a slab model) to extract the density profile [5–7]. In previous studies [3, 8], multiple contrast neutron measurements at room temperature had determined within  $\text{\AA}$  precision the profile of adsorbed and floating bilayers. The silicon is covered by a  $12 \pm 1 \text{ \AA}$  thick oxide. A thin water film of thickness  $d_W$  separates it from the adsorbed bilayer. Each bilayer is resolved into outer-inner-outer slabs: outer slab = heads (phospho-choline and glycerol groups), inner slab = tails (hydrocarbon chains). Within each bilayer, the thickness of the head regions is denoted by  $d_H$  and  $D_H$ , the thickness of the tail regions by  $d_T$  and  $D_T$  (the thicknesses of the whole bilayers by  $d_B$  and  $D_B$ ), for the adsorbed and floating bilayer, respectively. The water film of thickness  $D_W$  separates the adsorbed and floating bilayers. This amount to 9 slabs in total, each one having its own average thickness and scattering length density (“refractive index”). Moreover, each interface between two slabs has a certain width, also called r.m.s. roughness, denoted by  $\sigma_a$  and  $\sigma_f$  for the adsorbed and floating bilayer, respectively. Since they enter into the density profile, they can be determined by fits of reflectivity curves, but their physical origin is not made explicit: whether static intrinsic width, temporal or spatial fluctuations, averaged over the neutron beam’s  $\mu\text{m}$  correlation length.

TABLE I – Structural parameters (in  $\text{\AA}$ ) derived from model fitting the reflectivity profiles from the double bilayer at different temperatures. To facilitate comparison with the literature, we present the bilayer thicknesses obtained by fitting only the thickness of tails, each head slab thickness being kept fixed at  $9 \text{ \AA}$ . Scattering length densities (in  $10^{-6} \text{ \AA}^{-2}$ ) were taken as in [3, 8]: substrate (Si) = 2.07; oxide ( $\text{SiO}_2$ ) = 3.41; subphase ( $\text{D}_2\text{O}93\%$ ) = 5.85; stearyls chains ( $\text{C}_{34}\text{H}_{66}$ ) =  $-0.41$ ; head PC ( $\text{C}_{10}\text{H}_{18}\text{O}_8\text{PN}$ ) = 1.74; in addition, 15–20% vol.vol amount of  $\text{D}_2\text{O}$  in the heads and 5–10% vol.vol in tails account for head hydration [9, 10] and incomplete coverage. Incomplete rows: quick scans with only the first reflectivity minimum. Error bars: extreme values which fit the data.

$T \text{ (}^\circ\text{C)}$	$d_W$	$d_B$	$\sigma_a$	$D_W$	$D_B$	$\sigma_f$
25.4	$5 \pm 1$	$55 \pm 1$	$3 \pm 1$	$16 \pm 1$	$55 \pm 1$	$3 \pm 1$
41.8	$5 \pm 1$	$55 \pm 1$	$3 \pm 1$	$17 \pm 1$	$55 \pm 1$	$3 \pm 1$
51.5	$10 \pm 2$	$56 \pm 1$	$3 \pm 1$	$60 \pm 4$	$58 \pm 2$	$32 \pm 5$
52.5	$6 \pm 3$			$47 \pm 1$		
53.4	$5 \pm 1$			$21 \pm 1$		
54.4	$5 \pm 1$			$21 \pm 1$		
55.4	$5 \pm 1$	$55 \pm 1$	$3 \pm 2$	$21 \pm 1$	$49 \pm 1$	$4 \pm 1$
56.3	$5 \pm 1$			$22 \pm 1$		
57.3	$5 \pm 1$			$22 \pm 1$		
64.1	$5 \pm 1$	$45 \pm 1$	$5 \pm 2$	$27 \pm 1$	$45 \pm 1$	$11 \pm 2$

The present work focuses on thicknesses and roughnesses only; one lipid-water contrast is not enough to determine precisely the scattering length density  $\rho$  of the different layers. So we started from the above 9-slab model, with the tabulated values of  $\rho$  (see caption of table I [3,8]) and fitted the relevant parameters to the data (fig. 1). The first reflectivity minimum abscissa is especially sensitive to the thickness of both D<sub>2</sub>O films. The second reflectivity minimum position is mainly sensitive to the thicknesses of the tail slabs  $d_T$  and  $D_T$ . The amplitudes and sharpnesses of both minima indicate bilayer roughnesses  $\sigma_a$  and  $\sigma_f$ . All slabs were easily distinguished, except that the high hydration of lipid heads [9,10] prevents a localization of the head/D<sub>2</sub>O interface to better than 1 Å. The main results are summarized in table I. We thoroughly checked *a posteriori* that they are not sensitive to the model (as discussed in [7]), nor to values of head slab thickness or scattering length densities within physically reasonable ranges. In particular, correcting the scattering length densities for temperature variations had no significant effect on the positions of the reflectivity minima, hence on the fitted parameters.

At low temperatures, in the gel phase (fig. 1a), the system has the structure of two isolated bilayers consistent with [3]. At intermediate temperatures, the reflectivity curves drastically change (fig. 1b). A first coarse fitting of the data, starting from the gel phase model, shows that the changes, both in overall shape and in the position of the minima, are mainly due to an increase in both thicknesses and roughnesses. At high temperature (fig. 1c), the six-parameter fit is excellent again. All parameters decrease back to values similar to those related to the gel phase; except that the floating bilayer is slightly thinner and further from the adsorbed one. This is our first result of importance as a biomembrane model: the floating bilayer remains stable even in the fluid phase.

The second result is the surprising evolution at intermediate temperature. Repeated measurements checked that these curves are time independent. The fact that the curve in fig. 1c is similar to that in fig. 1a indicates that the sample has probably not been damaged. To exclude the possibility of an artifact requires control experiments with more samples, different molecules and water contrasts; preliminary analysis of repeated tests displays, indeed, the same behaviour, and in a reversible way. Only off-specular reflectivity could completely characterize them [11]; in fact, the Debye-Waller approximation for specular reflectivity [5] fails here. Thus we extensively used both deterministic and random fitting procedures to test the significance of the results (error bars of table I).

The adsorbed layer is barely affected, with a small increase of  $\sigma_a$  ( $\sim 4$  Å), and its thickness  $d_B$  is well determined by the sharp second minimum. On the other hand, the sharp first minimum determines the total thickness of the hydrophilic region  $d_H + D_W + D_H$ , which significantly increases. Note that, in multilamellar systems, such an increase in the total repeating distance (*i.e.*  $D_W + D_B$  in our notations) had already been observed around  $T_m$  and studied in detail [12]; however, since the increase was less than 5 Å, it was difficult to discriminate between a swelling of  $D_W$  [13–15], an increase in  $D_B$  due either to disorder in tails or hydration of heads [16], or multiple contributions [12].

In the present work, with a single floating bilayer, two arguments favor an increase in  $D_W$ . First, the observed effect is too large to be attributed to the bilayer: the tails barely thicken, and from the data (as well as intuitively) it is also hard to imagine that the heads thicken more than a few Å. Second, neutron reflectometry here distinguishes the hydrophilic region from the hydrophobic one. Even  $D_W$  itself is measured; its error bar is of course large (an increment in the value of  $D_W$  could be balanced by a twice larger decrement in less contrasted heads) but still not larger than  $\pm 4$  Å. Hence, the spectacular maximum in  $D_W$  and  $\sigma_f$  is significant. Can we explain it? We now discuss two possible interpretations.

First, this maximum in both thickness and roughness seems to occur near the pretransitional temperature  $T_p$ , rather than at the (main) melting temperature  $T_m$  (respectively,

$\approx 51\text{-}52^\circ\text{C}$  and  $\approx 55.0\text{-}55.1^\circ\text{C}$  for DSPC in  $\text{D}_2\text{O}$  [17,18]). This would be in agreement with the existence of a static ripple phase  $P_{\beta'}$  between  $T_p$  and  $T_m$  [19,20] which can lead to an increase of the water thickness. However, one would then expect that both bilayers acquire a large roughness, comparable to the inter-bilayer distance: this is not what we observe.

Second, we might be observing the balance between the undulation repulsion [21,22] and van der Waals attraction [2]. For the first time, the configuration, a bilayer floating in a semi-infinite space, is ideal for comparison with existing theories. There is no additional constraint coming from closed geometry, as in vesicles [23], or from confinement and coupled fluctuations, as in multi-lamellar systems [12–14,22,24,25]. When the bilayer-bilayer distance  $D_W$  is large, the interactions between neutral bilayers are likely to dominate the pinning on possible defects, the short-range ( $\lambda_H \sim 2\text{-}3 \text{ \AA}$ ) hydration force, and the repulsion of residual charges [26]. The r.m.s. roughness  $\sigma_f$  is large too, indicating that the bilayer is soft. A dimensionless parameter  $\beta = (k_B T)^2 / \kappa A$  characterizes this balance:  $\kappa$  is the bending modulus of the bilayer,  $A$  the Hamacker constant.

To determine the fluctuation-induced free energy as a function of  $\beta$  is a non-trivial task in this high- $D_W$ , high- $\sigma_f$  regime [27–29]. The central quantity  $\mu(\beta) = (\sigma_f / D_W)^2$  is constant, with estimated values of  $\mu = 1/6$ , 0.183 or  $1/4$  according to a heuristic argument, Monte Carlo simulation, or self-consistent numerical calculation, respectively [30,31]. A self-consistent theory (in progress) separates the short-wavelength fluctuations governed by bending rigidity, from the long-wavelength fluctuations determined by the hard-wall potential. Calculating self-consistently the total width  $\sigma_f$  within a Gaussian approximation in both Fourier and real

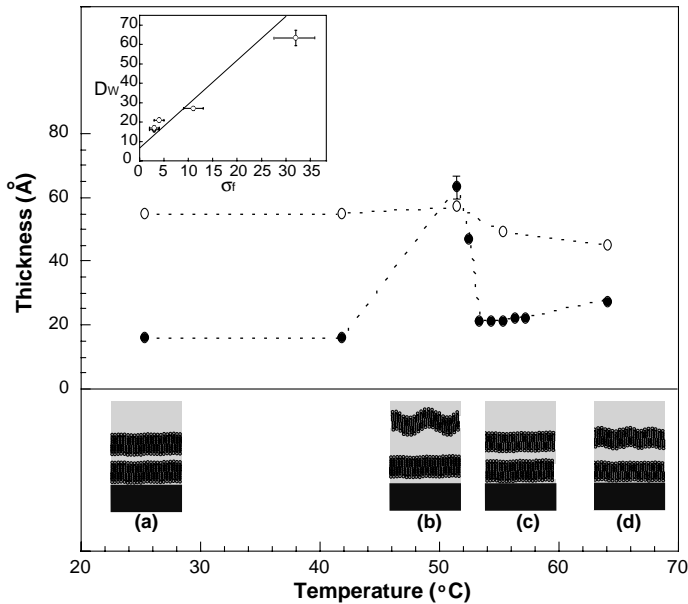


Fig. 2 – Top: bilayer thickness  $D_B$  (○) and inter-bilayer distance  $D_W$  (●) from table I, plotted *vs.* temperature; dots = guides for the eye. Insert:  $D_W$  *vs.* roughness  $\sigma_f$ ; solid line:  $D_W = 2.35 \sigma_f + 5 \text{ \AA}$ , see text. Bottom: schematic view drawn to scale along the vertical axis, (a) gel phase, (b) transition temperature, (c) fluid phase, (d) high temperature.

space, one finds that  $\mu$  depends on the in-plane correlation length  $\xi_{||}$  of the membrane. For a membrane between *two* hard walls, one obtains the value  $\mu \sim 1/5$  for rigid membrane ( $\xi_{||}$  larger than the microscopic length scale,  $\beta \ll 1$ ), and  $\mu \sim 1/3$  for soft membrane ( $\beta \gg 1$ ), in very good agreement with Monte Carlo simulations [32]. For a membrane held by van der Waals attraction near *one* hard wall, the self-consistent theory yields  $\mu(\beta) = \sigma_f^2 / (D_W - 2\lambda_H)^2$ . The steric repulsion potential is shifted towards larger distances due to the hydration forces (hence the term  $\lambda_H$ ) while the van der Waals attraction remains unaltered.

Eliminating  $\beta$  yields a relation between  $D_W$  and  $\sigma_f$ , robust to assumptions on the microscopic potential. For instance, assuming for simplicity the expression  $\sim A/D_W^2$  for van der Waals interactions, we obtain the approximate linear relation  $D_W \sim 2.35 \sigma_f + 2\lambda_H$ , in agreement with our data (fig. 2, insert).

On the other hand, at given  $\beta$ , the actual values of  $D_W$  and  $\sigma_f$  are very sensitive to details of the inter-bilayer interactions. Thus extracting the value of  $\beta$  from measurements of  $D_W$  and  $\sigma_f$  would be too model sensitive to be quantitative. Qualitatively, it seems that  $\beta$  strongly increases, approaching but never reaching the critical value for unbinding (of order unity). Assuming that  $A$  barely varies with  $T$  would imply that  $\kappa$  decreases to a few  $k_B T$  and increases again. This is consistent with the comparison between two recent measurements of  $\kappa$  for DMPC vesicles, one in fluid phase [33], and a more difficult one in gel phase [34]. Off-specular measurements of the fluctuation spectrum throughout the whole range of the transition region could directly test whether the increase in bilayer-bilayer distance is related to a lower bending modulus and higher fluctuations.

The physical origin, and even the existence of such minimum in  $\kappa$  is unclear in the literature. It would be tempting to attribute it to a phase transition within the bilayer. As already mentioned, for DSPC in  $D_2O$  the pretransition  $T_p \approx 51-52$  °C [17, 18] is close to the largest effect we observed. On the other hand, a minimum in  $\kappa$  would more likely be expected [14, 34] near the main (melting) transition  $T_m$ . This would imply that for the floating bilayer  $T_m$  is lower than the value  $\approx 55.0-55.1$  °C reported for totally free bilayers [17, 18]. A comparable lowering of the melting temperature has been previously observed on single bilayer on a solid support [35] and was attributed to surface tension effects. In our floating bilayer, a lateral stress might arise from possible pinning on defects. However, such a large tension would strongly limit the fluctuations and prevent both  $D_W$  and  $\sigma_f$  from increasing as much as we observe [27].

To summarize, a freely floating bilayer offers interesting advantages. a) For biophysics, having a structured bilayer, stable in time and free to fluctuate in fluid phase it enables *in situ* studies of transmembrane channels or interaction between a lipid bilayer and membrane proteins. Its size, orientation, and the proximity of a smooth substrate enable reflectivity studies. The composition of both lipids and surrounding medium can be chosen. b) For soft matter physics, this geometry enables a comparison with theoretical models; it also provides different control parameters (temperature, composition of lipids or water) to study the interaction between two membranes. For instance, thanks to the excess water, we have observed a large increase in both the free bilayer roughness and the inter-bilayer distance. It might be a direct observation of the balance between energy and entropic repulsion, and an evidence for a minimum in the bending modulus  $\kappa$ .

\* \* \*

We have benefitted from fruitful discussions with R. LIPOWSKY, R. NETZ, J. DAILLANT, A. BRASLAU and T. SALDITT.

## REFERENCES

- [1] MOURITSEN O. and ANDERSEN O. (Editors), *In Search of a New Biomembrane Model, Biologiske Skrifter 49* (The Royal Danish Academy of Sciences and Letters, Copenhagen) 1998.
- [2] LIPOWSKY R., *Handbook of Biological Physics*, edited by R. LIPOWSKY and E. SACKMANN, Vol. 1 (Elsevier Science) 1995, p. 521.
- [3] CHARITAT T., BELLET-AMALRIC E., FRAGNETO G. and GRANER F., *Eur. Phys. J. B*, **8** (1999) 583.
- [4] TAMM L. K. and MCCONNELL H. M., *Biophys. J.*, **47** (1985) 105.
- [5] PENFOLD J. and THOMAS R. K., *J. Phys. Condens. Matter*, **2** (1990) 1369.
- [6] JOHNSON S. J., BAYERL T. M., MCDERMOTT D. C., ADAM G. W., RENNIE A. R., THOMAS R. K. and SACKMANN, E., *Biophys. J.*, **59** (1991) 289.
- [7] KOENING B. W., KRUEGER S., ORTS W. J., MAJKRZAK C. F., BERK N. F., SILVERTON J. V. and GAWRISCH K., *Langmuir*, **12** (1996) 1343.
- [8] FRAGNETO G., GRANER F., CHARITAT T., DUBOS P. and BELLET-AMALRIC E., *Langmuir*, **16** (2000) 4581.
- [9] JENDRIASAK G. and HASTY J., *Biochim. Biophys. Acta*, **337** (1974) 79.
- [10] SUN W. J., SUTTER R. M., KNEWTSON M. A., WORTHINGTON C. R., TRISTRAM-NAGLE S., ZHANG R. and NAGLE J. F., *Phys. Rev. E*, **49** (1994) 4665.
- [11] BELLET-AMALRIC E., BRASLAU A., CHARITAT T., DAILLANT J., FRAGNETO G., GRANER F. and PERINO-GALLICE L., in preparation.
- [12] NAGLE J. F., PETRACHE H. I., GOULIAEV N., TRISTAM-NAGLE S., LIU Y., SUTER R. M. and GAWRISCH K., *Phys. Rev. E*, **58** (1998) 7769.
- [13] CHEN F. Y., HUNG W. C. and HUANG H. W., *Phys. Rev. Lett.*, **79** (1997) 4026.
- [14] LEMMICH J., MORTENSEN K., IPSEN J. H., HØNGER T., BAUER R. and MOURITSEN O. G., *Phys. Rev. E*, **53** (1996) 5169.
- [15] LEMMICH J., MORTENSEN K., IPSEN J. H., HØNGER T., BAUER R. and MOURITSEN O. G., *Phys. Rev. Lett.*, **75** (1995) 3958.
- [16] ZHANG R., SUN W., TRISTAM-NAGLE S., HEADRICK R. L., SUTER R. M. and NAGLE J. F., *Phys. Rev. Lett.*, **74** (1995) 2832.
- [17] GUARD-FRIAR D., CHEN C. H. and ENGLE A. S., *J. Phys. Chem.*, **89** (1985) 1810.
- [18] OKHI K., *Biochem. Biophys. Res. Commun.*, **174** (1991) 102.
- [19] FANG Y. and YANG J., *J. Phys. Chem.*, **100** (1996) 15614.
- [20] HEIMBURG T., *Biophys. J.*, **78** (2000) 1154.
- [21] HELFRICH W., *Z. Naturforsch. A*, **30** (1978) 305.
- [22] ABILLON O. and PEREZ E., *J. Phys. (Paris)*, **51** (1990) 2543.
- [23] EVANS E. and RAWICZ W., *Phys. Rev. Lett.*, **64** (1990) 2094.
- [24] SAFINYA C., SIROTA E., ROUX D. and SMITH G., *Phys. Rev. Lett.*, **62** (1989) 1134.
- [25] VOGEL M., MÜNSTER C., FENZL W. and SALDITT T., *Phys. Rev. Lett.*, **94** (2000) 390.
- [26] PINCET F., CRIBIER S. and PEREZ E., *Eur. Phys. J. B*, **11** (1999) 127.
- [27] LIPOWSKY R. and LEIBLER S., *Phys. Rev. Lett.*, **56** (1986) 2541.
- [28] LIPOWSKY R., *Z. Phys. B*, **97** (1995) 193.
- [29] MILNER S. T. and ROUX D., *J. Phys. I*, **2** (1992) 1741.
- [30] JANKE W. and KLEINERT H., *Phys. Lett. A*, **117** (1986) 353.
- [31] PODGORNİK R. and PARSEGIAN A., *Langmuir*, **8** (1992) 557.
- [32] GOMPPER G. and KROLL D., *Europhys. Lett.*, **9** (1989) 59.
- [33] MÉLÉARD P., GERBAUD C., POTT T., FERNANDES-PUENTE L., BIVAS I., MITOV M., DUFOURCQ J. and BOTHOREL P., *Biophys. J.*, **72** (1997) 2616.
- [34] DIMOVA R., POULIGNY B. and DIETRICH C., *Biophys. J.*, **79** (2000) 340.
- [35] NAUMAN C., BRUMM T. and BAYERL T. M., *Biophys. J.*, **63** (1992) 1314.